Figure S1. Effect of etomoxir-treated-GC-MSCs and etomoxir-treated-BM-MSCs with circ_0024107 overexpression on gastric cancer cell invasion. (A) Representative images of the invaded gastric cancer cells following incubation with CM from etomoxir-treated GC-MSCs. (B) Representative images of the invaded gastric cancer cells following culture with CM from etomoxir-treated BM-MSCs with circ_0024107 overexpression. Scale bars, 100 μM; magnification, x200. circRNA, circular RNA; GC-MSCs, gastric cancer-derived mesenchymal stem cells; BM-MSCs, bone marrow-derived mesenchymal stem cells; CM, conditioned medium; ETO, etomoxir.

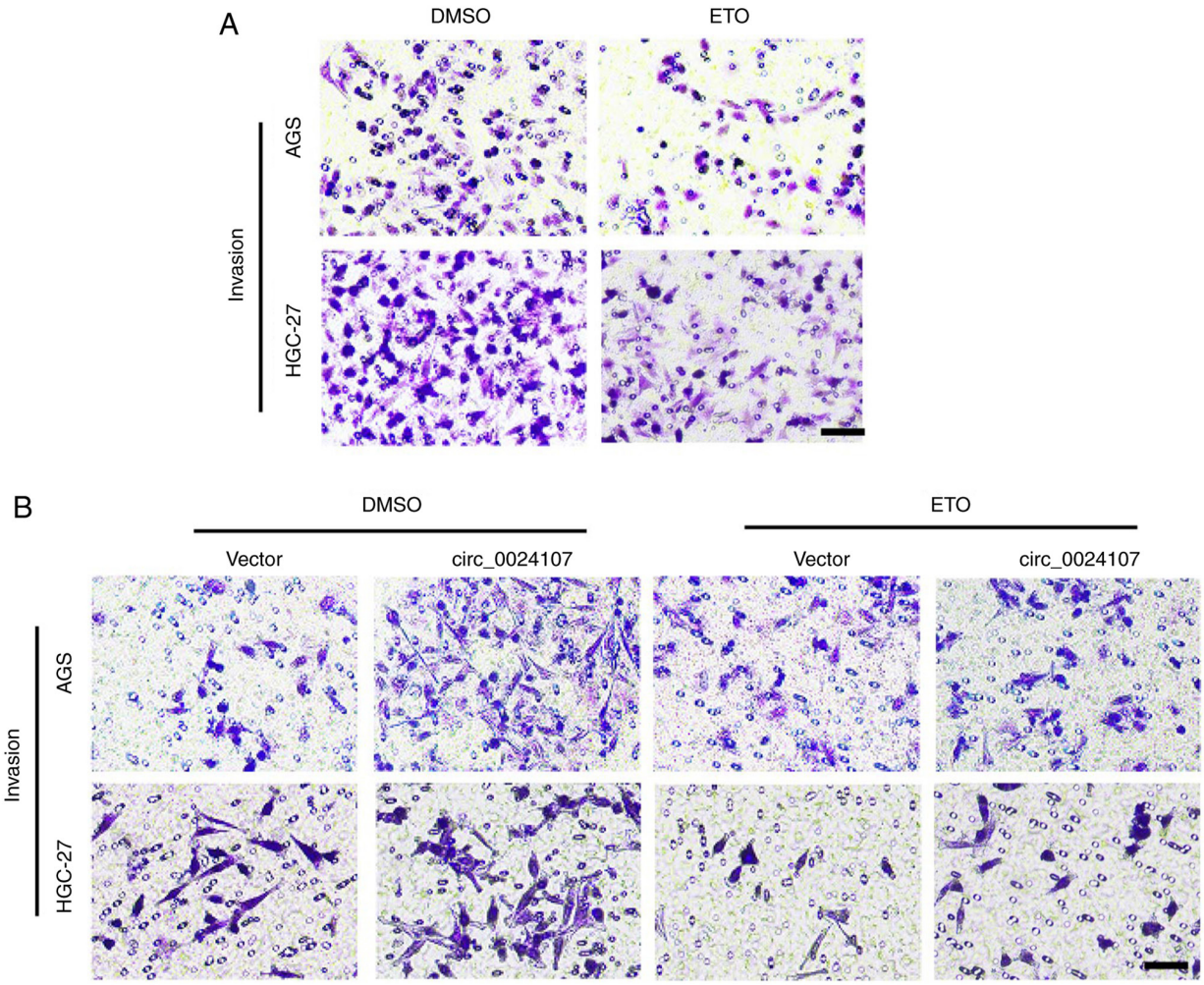

Figure S2. Effect of miRNA mimic-transfected GC-MSCs, inhibitor-transfected BM-MSCs and etomoxir-treated BM-MSCs in which miRNAs were silenced on gastric cancer cell invasion. (A and B) Representative images of the invaded gastric cancer cells following incubation with CM from (A) miRNA mimic-transfected GC-MSCs and (B) inhibitor-transfected BM-MSCs. (C) Representative images of the invaded gastric cancer cells following incubation with CM from etomoxir-treated BM-MSCs and in which the two miRNAs were silenced. Scale bars, 100 μM; magnification, x200. GC-MSCs, gastric cancer-derived mesenchymal stem cells; BM-MSCs, bone marrow-derived mesenchymal stem cells; CM, conditioned medium; ETO, etomoxir.

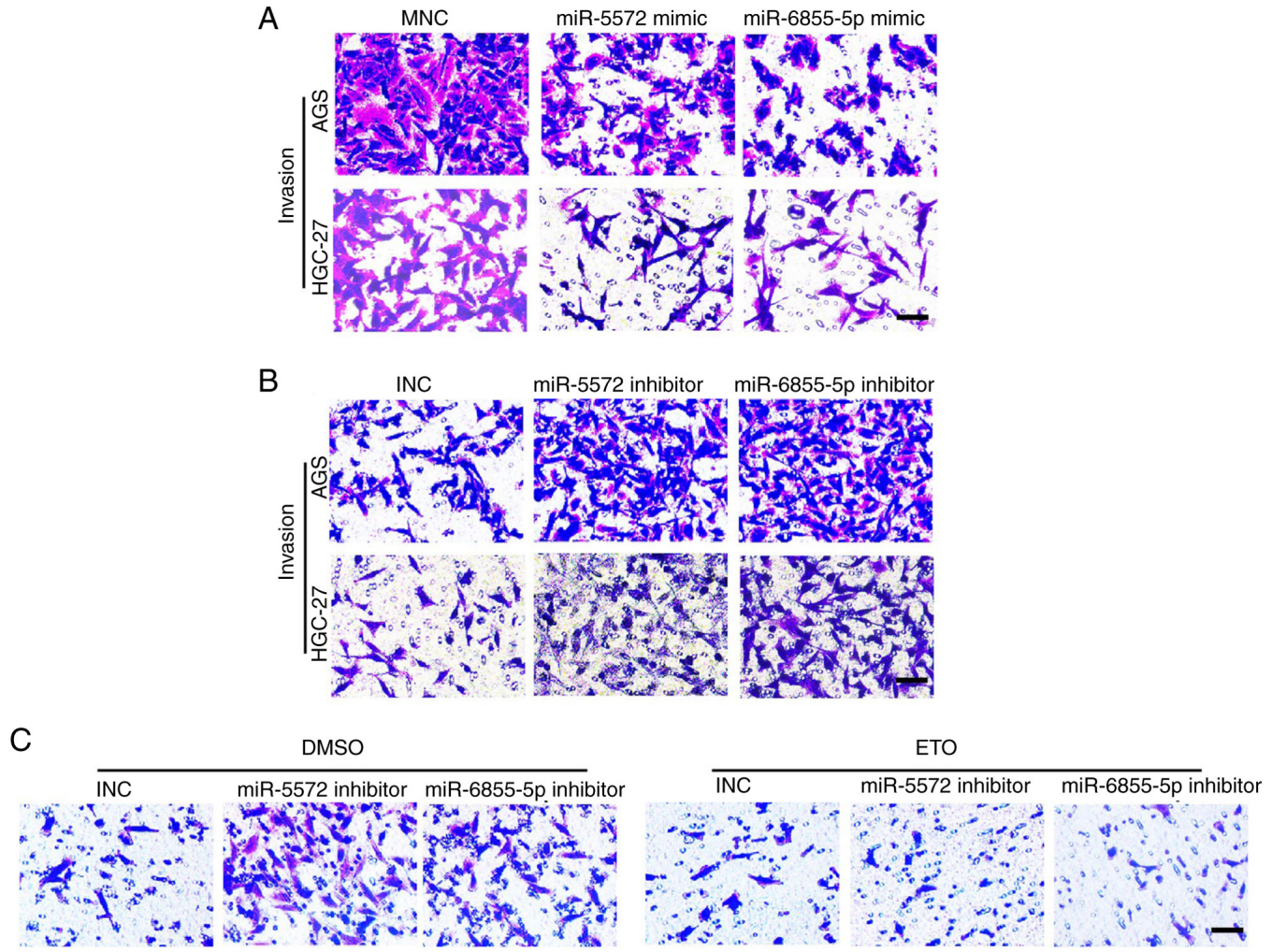

Figure S3. Effects of circ_0024107 knockdown on the migratory and invasive capacities, CPT1A expression, FAO activity and miRNA expression of HGC-27 cells. (A) RT-qPCR analysis of circ_0024107 in HGC-27 cells following transfection with siRNAs against circ_0024107. (B and C) Migration and invasion analysis. Detection of CPT1A (D) mRNA (E) and protein levels. (F and G) FAO activity detection. (H) RT-qPCR analysis of miR-5572 and miR-6855-5p expression. Scale bars, 100 μM; magnification, x200. Values are presented as the mean ± SD (n=3). **P<0.01 and ***P<0.001, vs. respective control. circRNA, circular RNA; CPT1A, carnitine palmitoyltransferase 1A; FAO, fatty acid oxidation; RT-qPCR, reverse transcription-quantitative PCR.

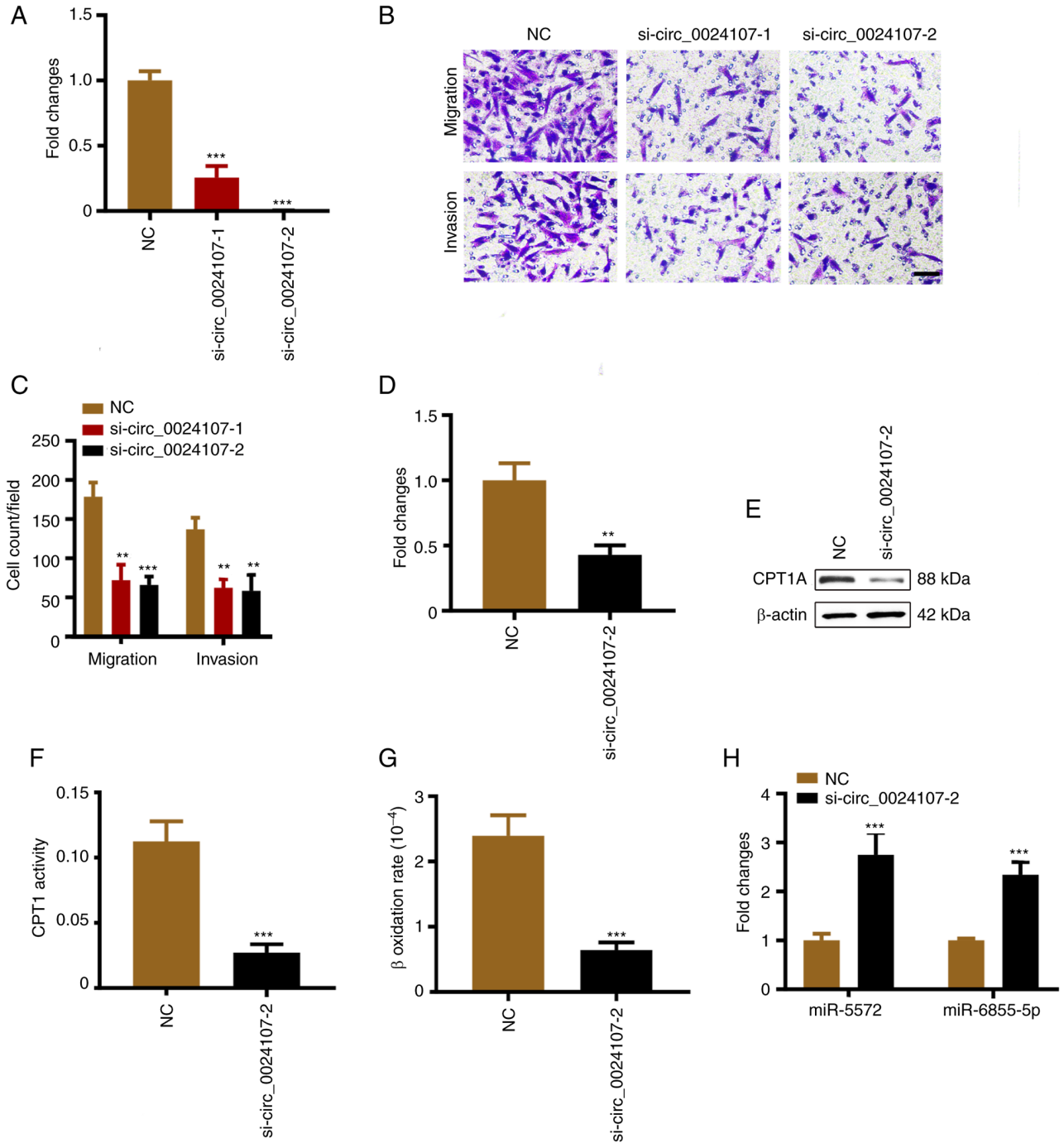

Figure S4. Effects of miR-5572 and miR-6855-5p overexpression on CPT1A expression, FAO activity, and the migratory and invasive capacities of HGC-27 cells. Detection of CPT1A (A) mRNA and (B) protein levels in HGC-27 cells following transfection with miRNA mimics. (C and D) FAO activity detection. (E and F) Migration and invasion analysis. Scale bars, 100 μM; magnification, x200. Values are presented as the mean ± SD (n=3). ***P<0.001, vs. respective control. CPT1A, carnitine palmitoyltransferase 1A; FAO, fatty acid oxidation; MNC, miRNA mimics negative control.

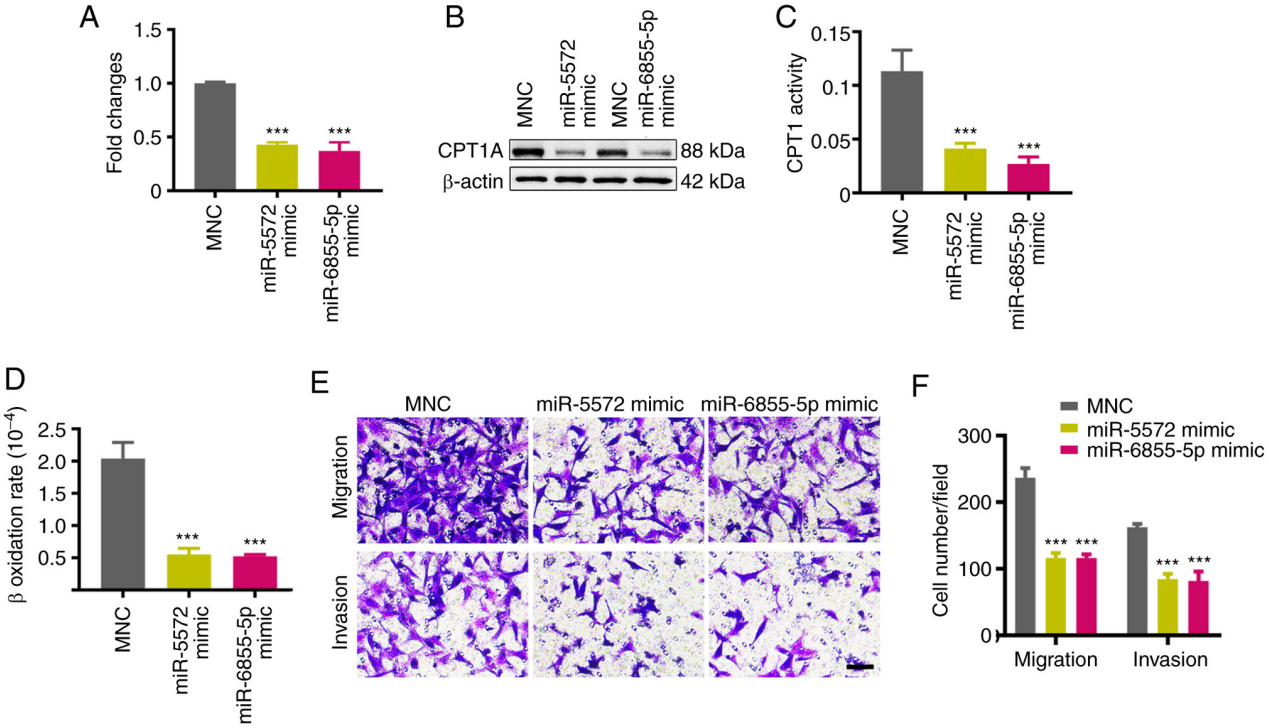

Figure S5. Correlation analysis of molecules involved in the circ_0024107/miR-5572/6855-5p/CPT1A axis in both of GC-MSCs and BM-MSCs. Scatter plots of the correlation between (A) circ_0024107 and CPT1A, (B) miR-5572 and CPT1A, (C) miR-6855-5p and CPT1A, (D) circ_0024107 and miR-5572, and (E) circ_0024107 and miR-6855-5p. Values are presented as the mean (n=3) circRNA, circular RNA; GC-MSCs, gastric cancer-derived mesenchymal stem cells; BM-MSCs, bone marrow-derived mesenchymal stem cells; CPT1A, carnitine palmitoyltransferase 1A.